HHS Public Access

Author manuscript

Nat Chem Biol. Author manuscript; available in PMC 2013 May 01.

Published in final edited form as:

Nat Chem Biol. 2012 November ; 8(11): 926–932. doi:10.1038/nchembio.1087.

A RubisCO like protein links SAM metabolism with isoprenoid biosynthesis

Tobias J. Erb[1,2,*,§], **Bradley S. Evans**[1,3,*], **Kyuil Cho**[1,3], **Benjamin P. Warlick**[1,2], **Jaya Sriram**[4], **B. McKay Wood**[1], **Heidi J. Imker**[1], **Jonathan V. Sweedler**[1,3], **F. Robert Tabita**[4], and **John A. Gerlt**[1,2,3]

[1]Institute for Genomic Biology, University of Illinois at Urbana-Champaign

[2]Department of Biochemistry, University of Illinois at Urbana-Champaign

[3]Department of Chemistry, University of Illinois at Urbana-Champaign

[4]Department of Microbiology, The Ohio State University

Abstract

Functional assignment of uncharacterized proteins is a challenge in the era of large-scale genome sequencing. Here, we combine *in extracto*-NMR, proteomics, and transcriptomics with a newly developed (knock-out) metabolomics platform to determine a potential physiological role for a ribulose-1,5-bisphosphate carboxylase/oxygenase (RubisCO)-like protein (RLP) from *Rhodospirillum rubrum*. Our studies unravelled an unexpected link in bacterial central carbon metabolism between *S*-adenosylmethionine (SAM)-dependent polyamine metabolism and isoprenoid biosynthesis and also provide an alternative approach to assign enzyme function at the organismic level.

D-Ribulose-1,5-bisphosphate carboxylase/oxygenase (RubisCO) is the most abundant protein in the biosphere and catalyzes the key reaction in the Calvin-Benson-Bassham cycle, the major process of atmospheric CO_2 fixation on earth[1,2]. To date, three different types of RubisCO are distinguished that all serve as true carboxylases in plants, bacteria, and archaea, respectively. However, recent sequencing projects identified RubisCO homologs (RubisCO-like proteins, RLPs) in a number of bacterial and archaeal genomes, such as *Chlorobaculum tepidum*, *Bacillus subtilis*, *Pseudomonas putida*, *Mesorhizobium loti*, *Archaeoglobus fulgidus*, and *Rhodospirillum rubrum*[2]. In contrast to true RubisCOs, RLPs

[*]These authors contributed equally to this work.

[§]Current address Institute for Microbiology, ETH Zurich, Switzerland.

Author contributions

T.J.E., B.S.E., and J.A.G. conceived and designed the experiments. T.J.E. performed the experiments with exception of metabolome analyses that were acquired by B.S.E., K.C., and B.M.W., as well as biochemical characterization of the cupin protein *in vitro* that was performed by B.S.E, and B.P.W. B.S.E., K.C., B.M.W., and J.V.S. developed the mass spectrometric platform and evaluated mass spectrometric data. J.S. and F.R.T. created and provided the *rlp*-and *cupin*-mutant strains of *R. rubrum*. B.P.W. and H.J.I. provided chemicals and recombinant enzymes for the synthesis of chemicals. T.J.E. and J.A.G. wrote the paper.

Competing financial interests

The authors declare no competing financial interests.

lack essential, conserved active site residues. Consequently, none of these proteins tested so far has been shown to catalyze the carboxylation of *D*-ribulose-1,5-bisphosphate.

Given the importance of RubisCO in the global carbon cycle, much effort has been undertaken to understand the evolutionary relationship and functional diversity within the RubisCO-superfamily and its RLP members[3–5]. Based on phylogenetic analysis, active site differences and genome context, at least six different RLP-subfamilies were identified that are assumed to use different substrates and catalyze different reactions (Fig. 1a)[2]. However, correct functional assignments of RLPs are hampered by the fact that *i*) RubisCO itself is already an inefficient, naturally promiscuous enzyme[6–8], and *ii*) potential substrate libraries of phosphorylated metabolites are not easily accessible. Although initial studies on the *Chlorobium tepidum* RLP-subfamily had established that RLPs might be involved in some aspect of sulfur metabolism[3], the only group of RLPs for which an exact physiological function has been determined is the *Bacillus subtilis* RLP-subfamily[4,9,10]. RLPs in this group catalyze an enolization reaction in a bacterial variation of the ubiquitous “methionine salvage pathway” that converts 5′-methylthio-adenosine (MTA), a dead-end product of SAM-dependent polyamine biosynthesis, into *L*-methionine [4,11,12] (Fig. 1b).

Earlier experiments on the *R. rubrum* RLP indicated that this enzyme also functions in MTA metabolism. Wild type *R. rubrum* can grow with MTA as sole source of sulfur; however, disruption of the RLP gene results in a MTA-deficient growth phenotype under aerobic conditions[13]. Moreover, when incubated *in vitro* with 5-methylthio-D-ribulose-1-phosphate (MTRu-1P), an intermediate of the canonical methionine salvage pathway, recombinant *R. rubrum* RLP was shown to catalyze an unprecedented 1,3-isomerization reaction (presumably two successive 1,2-isomerization reactions) to yield a 1:3 mixture of 1-methylthio-ribulose-5-phosphate (MTRu-5P) and 1-methylthio-xylulose-5-phosphate (MTXu-5P) [5]. However, despite these apparent links to MTA metabolism, we noticed that the *R. rubrum* genome lacks most of the canonical methionine salvage pathway genes and, therefore, might use an alternative strategy to utilize MTA aerobically as its sole sulfur source. In addition, the physiological context of the non-stereospecific isomerization reaction observed with recombinant RLP *in vitro* remained enigmatic to us.

In this study, we combined *in extracto*-NMR, transcriptomics, proteomics, classical biochemical methods and genetic knock-outs together with a newly developed metabolomics platform to elucidate MTA metabolism in *R. rubrum*. Our results give evidence for a so far unknown central metabolic pathway, involving *R. rubrum* RLP, in which the polyamine biosynthesis dead-end product MTA is channelled into isoprenoid metabolism with concomitant release of the volatile gas methanethiol. The proposed MTA-isoprenoid pathway fits to the organism’s physiology and phylogenetic analysis indicate that a number of organisms make use of this metabolic shunt.

RESULTS

In extracto-NMR unravels initial steps of MTA metabolism

In order to elucidate the unknown MTA metabolic pathway in *R. rubrum*, we first used ^{1}H-NMR to trace the fate of MTA in *R. rubrum* cell extracts (*in extracto*-NMR). For that

purpose, extracts of *R. rubrum* were prepared from cells actively growing with MTA as sole sulfur source (generation time t_d=16.7 ± 3.0 h). Then, these extracts were exchanged into buffered D_2O, MTA was added and ^{1}H-NMR spectra were continuously recorded over time (Supplementary Results, Supplementary Fig. 1). MTA was first converted into 5-methylthio-*D*-ribose-1-phosphate (MTR-1P) with the release of adenine. Subsequently, MTR-1P was isomerized into MTRu-1P (Fig. 2). The overall rate for this reaction sequence (0.7 + 0.3 nmol min^{-1} mg^{-1} protein) closely matched the theoretically expected minimal activity for MTA metabolic enzymes (0.6 nmol min^{-1} mg^{-1}) to sustain the observed growth of *R. rubrum*, as calculated from the specific aerobic growth rate of *R. rubrum* on MTA (μ=0.042 + 0.008h^{-1}, Supplementary Fig. 1). Notably, we could demonstrate MTRu-1P formation at comparable rates also in extracts of sulfate-grown cells, suggesting that MTA metabolism serves a housekeeping function in *R. rubrum*, analogous to the reactions of the classical methionine salvage pathway in *B. subtilis*[14–16]. However, in neither extract could metabolites downstream of MTRu-1P be detected by ^{1}H-NMR, indicating that further investigations are limited by the *in extracto* NMR-method used.

LC-FTMS metabolomics identifies an MTA-isoprenoid shunt

To identify subsequent reactions steps in MTA metabolism by *R. rubrum* we developed a liquid-chromatography Fourier transform mass spectrometry (LC-FTMS)-based metabolomics platform that would allow a comprehensive analysis of the *R. rubrum* metabolome upon perturbation with MTA. This platform combines high-resolution mass spectrometry with new semi-automated data analysis tools for the customized, convenient and highly confident assignment of metabolites based on molecular formula determination (see Methods). To find metabolites specifically affected by MTA-perturbation, suspensions of *R. rubrum* cells actively growing on minimal medium with sulfate as sole sulfur source were shortly deprived in sulfur-free medium (10 min), before they were transferred onto minimal medium with or without MTA as sole sulfur source and incubated for 10, and 20 min, respectively. Then, metabolites were extracted from whole cells and analyzed by the LC-FTMS platform, as shown in Supplementary Figure 2. Of the 1,406 individual peaks observed from extracts of wild type *R. rubrum*, we identified a total of 25 metabolites (1.8%) that were significantly up-regulated in MTA-fed cells (Supplementary Table 1). In agreement with the *in extracto*-NMR results, three of the peaks unique to MTA-feeding could be assigned to MTA, MTR-1P, and MTRu-1P, respectively, and were experimentally confirmed by spiking cell extracts with authentic standards (Supplementary Fig. 3). An additional peak (hypoxanthine) could be assigned as an intermediate in bacterial purine metabolism, which is well in line with downstream metabolism of adenine following its release from MTA upon MTR-1P formation. However, much to our surprise three peaks were significantly up-regulated upon feeding of MTA that could be assigned as metabolites of isoprenoid biosynthesis: 1-deoxyxylulose-5-phosphate (DXP), 4-(cytidine-5′-diphospho)-2-*C*-methyl-*D*-erythritol (CDP-ME), and 2-*C*-methyl-*D*-erythritol-2,4-cyclodiphosphate (*c*-MEPP). Spiking of cell extracts with standards confirmed these assignments, indicating an unexpected intertwining of MTA metabolism and isoprenoid biosynthesis in *R. rubrum* (Supplementary Fig. 2). Realizing structural similarities between MTRu-1P and DXP, we hypothesized that DXP is a downstream metabolite of MTA, which is formed by release of the volatile methanethiol (CH_3SH) from an intermediate in the

pathway. Indeed, DXP formation in *R. rubrum* increased in a time dependent manner following MTA-feeding (Fig. 3a) as did the release of methanethiol in supernatants of *R. rubrum* cell suspensions (quantified with 5,5′-dithiobis(-2-nitrobenzoic acid, DTNB[17], Fig. 3b). The rate of methanethiol release from MTA-fed cells (4 nmol min^{-1} OD_{578}^{-1}) was independent of the sulfur source used to grow *R. rubrum* (Supplementary Fig. 4), again indicating that MTA metabolism is a housekeeping function in this organism. Finally, when testing a RLP disruption strain[13], we could neither observe an increase in DXP formation nor in methanethiol release, which confirmed the functional link between MTA metabolism and isoprenoid biosynthesis (Fig. 3c, 3d).

Knock-out metabolomics confirm the MTA-isoprenoid shunt

Next, we sought to identify genes important in MTA metabolism. By screening 10,200 transposon mutants of *R. rubrum* we identified four mutants in three genes that had lost the ability to release methanethiol upon MTA feeding (Supplementary Fig. 5), one of which was a mutant of the RLP gene (*rru_A1998*). The other two genes encode a putative MTA-phosphorylase (*rru_A0361*) and a putative MTR-1P isomerase (*rru_A0360*). Homologs of the three genes are conserved across the genomes of many bacterial species, where they are often organized as two distinct clusters (Supplementary Table 2). One cluster typically consists of the putative MTA-phosphorylase and the putative MTR-1P isomerase, whereas the second cluster comprises the RLP that is in many cases adjacent to a conserved gene encoding a small metal binding protein (*cupin*). Based on this observation, we consequently also created a *cupin* disruption strain. None of the mutant strains released methanethiol and consequently also did not show an increase in DXP-formation after MTA feeding, as demonstrated by LC-FTMS metabolomics (Fig. 3c, 3d). LC-FTMS metabolomic analysis enabled an even more detailed picture of each mutant that allowed functional assignments of the corresponding enzymes. The *rru_A0361*-mutant did not form MTR-1P or any other downstream metabolite, confirming its role as putative MTA-phosphorylase. MTA-metabolism in the *rru_A0360*-mutant stopped at the level of MTR-1P, according to its proposed role as MTR-1P-isomerase[13]. The *rru_A1998 (rlp)*-mutant accumulated MTRu-1P, as expected from the function of the RLP as an MTRu-1P isomerizing enzyme[5]. Finally, the *cupin*-mutant accumulated a mixture of MTRu-5P and MTXu-5P, affirming the role of RLP as MTRu-1P isomerase, and the cupin as being involved in processing these molecules (Fig. 3c, Supplementary Fig. 6). Based on these data, we propose the existence of a new bacterial pathway, the MTA-isoprenoid shunt that links SAM-dependent polyamine metabolism and isoprenoid biosynthesis, as summarized in Fig. 4. In this pathway, MTA, which is derived from polyamine biosynthesis, is first transformed into MTR-1P. MTR-1P is further isomerized to MTRu-1P, which then serves as substrate for the RLP. Due to the combined action of the RLP and the cupin protein, methanethiol is released, the phosphorylated ketose-coproduct is converted into DXP and further channeled into isoprenoid biosynthesis. Note that this proposed reaction sequence is also well supported by MTA-feeding metabolomics of *R. rubrum* wild type that showed the increase of all major metabolites of the proposed MTA-isoprenoid shunt over time, compared to (non-fed) control cells (Fig. 4).

Although our MTA-feeding (knock-out) metabolomics approach established the functional link between methanethiol release and DXP formation, and consequently the existence of the MTA-isoprenoid shunt, we still worried about the physiological relevance of this pathway *in vivo* in the absence of exogenous added MTA. For that purpose the metabolomes of *R. rubrum* wild type cells and mutants that had been grown on minimal medium with sulfate as sole sulfur source were analyzed for metabolites of the proposed MTA-isoprenoid shunt. Wild type *R. rubrum* contained some MTA-derived metabolites (*i.e.*, MTR-1P), but only at a very low level. This is expected[12], as metabolic flux through this pathway is small, because sulfur makes only up to 1.5% of the cellular dry mass[18], and spermidine is synthesized at low rates[19]. In contrast, levels of MTA-derived metabolites were approximately 50 times higher in *R. rubrum* mutants than in wild type, indicating accumulation of metabolites in the mutants, with individual patterns resembling those of the MTA-feeding experiments (Fig. 5). Notably, when grown with sulfate as sole sulfur source, the mutant strains appeared slightly less colored than wild type *R. rubrum* and had a lowered carotenoid content (Supplementary Fig. 7), indicating that isoprenoid biosynthesis is indeed fueled to some extent from MTA *in vivo*. In summary our results suggested that the proposed MTA-isoprenoid shunt is active *in vivo* and does not require addition of external MTA.

Biochemistry of methanethiol release and DXP-formation

To confirm the biochemistry of the MTA-isoprenoid shunt, we expressed the proteins of the proposed pathway heterologously (Supplementary Fig. 8) and tested their activity *in vitro*. Rru_A0360 and Rru_A0361 were successfully confirmed as *bona fide* MTA-phosphorylase and MTR-1P-isomerase, respectively (Supplementary Table 3), whereas the RLP reaction had been demonstrated previously[5]. Initial experiments to reconstitute the complete methanethiol-releasing reaction sequence *in vitro* failed. Any efforts to monitor methanethiol release by ^{1}H-NMR with purified proteins (Rru_A0360, RruA_0361, RLP and cupin) from MTA, or MTR-1P were unsuccessful, as were experiments in which methanethiol formation was assayed with *O*-acetyl*L*-homoserine sulfhydrylase (see below). Similarly, when we incubated purified cupin with the products of the RLP reaction (MTXu-5P/MTRu-5P) we could neither observe methanethiol release nor DXP formation by ^{1}H-NMR or mass spectrometry, indicating that an essential factor might be missing in these experiments. However, when we provided DTT to the reaction mixture, purified cupin was able to release methanethiol preferably from MTXu-5P yielding DXP, as shown by ^{1}H-NMR and LC-FTMS (Supplementary Fig. 9 and 10). This reaction was dependent on both the presence of cupin and stoichiometric amounts of DTT to go to completion, suggesting an unprecedented reductive release of the methanethiol group, that differs from other thiol releasing reactions described so far (*e.g.*, the elimination of homocysteine from *S*-ribosylhomocysteine in the biosynthesis of the quorum sensing-molecule AI-2[20]).

In summary, our results demonstrated the functionality of the proposed MTA-isoprenoid shunt with purified enzymes *in vitro*. Yet, we wondered about the relevance of this reaction sequence *in vivo*, *i.e.*, in the absence of external added reducing equivalents. We therefore developed an assay to monitor the release of methanethiol from MTR-1P, in which extracts of wild type or mutant *R. rubrum* cells were incubated with MTR-1P (or MTA) and the

volatile methanethiol was trapped with a DTNB-soaked filter paper. For wild type extracts, release of methanethiol from MTR-1P was quantified as 0.3 μM min^{-1} mg^{-1}, whereas methanethiol releasing activity was negligible in mutant cell extracts. However, methanethiol release in extracts of individual mutants could be successfully restored by addition of the respective missing enzyme. These experiments established the role of each protein in methanethiol release, eliminated the possibility of polar effects from mutagenesis, and confirmed the presence of an appropriate reducing equivalent *in vivo* (Supplementary Fig. 11).

Final steps in MTA metabolism: Recycling of methanethiol

Finally, to identify reactions and enzymes following the release of methanethiol, we compared the proteomes of MTA- and sulfate-grown cells. Five proteins were identified that were highly up-regulated during growth on MTA as sole sulfur source (Supplementary Table 4); among these were two putative *O*-acetyl-homoserine sulfhydrylases (Rru_A0774, Rru_A0784). Notably, four of these five proteins (Rru_A0779, Rru_A0792, and the two sulfhydrylases) were encoded by the same genetic region of fourteen different genes presumably involved in thiol metabolism at the level of cysteine and methionine ("thiol cluster", Fig. 6). A complementary transcriptome analysis using mRNA sequencing confirmed the results of the proteomic study and allowed a more detailed view on the differences between MTA- and sulfate-grown cells. Whereas the relative transcript levels of the majority (>99%) of the 3933 annotated genes of *R. rubrum* remained essentially unchanged for both conditions, including the genes involved in methanethiol release in agreement with their housekeeping function, the relative levels of transcripts for all fourteen genes of the "thiol cluster" were increased between 30- and 320-fold in MTA-grown cells (Supplementary Table 5, Fig. 6). Although this expression pattern resembled a generalized stress response by sulfur deprivation, we realized that expression of the "thiol cluster" and its putative *O*-acetyl-*L*-homoserine sulfhydrylases would provide *R. rubrum* with the metabolic capability to recapture methanethiol in the form of methionine, as reported recently[21,22]. Indeed, biochemical characterization of heterologously expressed Rru_A0774 confirmed the enzyme as methanethiol-specific *O*-acetyl-*L*-homoserine sulfhydrylase (Supplementary Table 3). This closed the gap between methanethiol release and methionine formation, explaining how *R. rubrum* recycles methanethiol when grown with MTA as sole sulfur source (Fig. 4).

DISCUSSION

In conclusion, our results give evidence for the existence of two so far unknown pathways in bacterial central metabolism: first, methanethiol release from MTA represents an alternative strategy to metabolize the dead-end product MTA besides the classical methionine salvage pathway[4,11,12]. At the same time, conversion of the remaining portion of MTRu-1P into DXP represents a new biosynthetic route to this isoprenoid precursor as an alternative to the well characterized non-mevalonate[23,24] pathway that prevails in many bacteria. Although *R. rubrum* encodes DXP synthase (Rru_A1592), the key enzyme of the non-mevalonate pathway that might provide most of the DXP in *R. rubrum*, the MTA-isoprenoid shunt, as proposed here, could also contribute to DXP biosynthesis. It is known that the major

polyamine produced by *R. rubrum* is spermidine[25,26], which requires the organism to cope with the dead-end product MTA that is formed from SAM during spermidine biosynthesis. Since the majority of pigments in the purple-colored non-sulfur bacterium *R. rubrum* are carotenoid-based, we note that the biosynthetic shunt described here, would fit very well to the organism's physiology because it allows the functional coupling of two biologically important processes in *R. rubrum*, polyamine biosynthesis and isoprenoid metabolism. As a matter of fact, carotenoid quantification experiments indicate up to 10% differences between aerobically grown *R. rubrum* wild type cells and MTA-isoprenoid shunt mutants (Supplementary Fig. 7). However, how much DXP exactly is synthesized via this metabolic shunt in *R. rubrum* remains to be investigated.

Phylogenetic analysis suggests that the MTA-isoprenoid shunt is not restricted to *R. rubrum*. *R. rubrum* RLP and related sequences (Supplementary Table 6) form a distinct branch in the cladogram that is well separated from RubisCOs type I–III, or other defined RLP groups[2] (Fig. 1), indicating a similar physiological function. A detailed analysis of more than 30 genomes confirm that almost all organisms harboring a *R. rubrum* RLP homolog also show the genetic potential to reductively release methanethiol from MTA analogous to the reaction sequence proposed here (Supplementary Table 2). This is further supported by the observation that in many of these organisms, MTA-phosphorylase and MTR-1P isomerase, on the one hand, and RLP and cupin, on the other hand are encoded by the same genomic region (or represent protein fusions). However, in some cases, MTA-phosphorylase is functionally replaced by a 5′-methylthioribose kinase homolog, or (phospho)-hydrolytic enzymes indicating that the initial steps that produce MTR-1P (from MTA or a similar substrate) might differ slightly, as seen for the classical methionine salvage pathway[11,27]. Similarly, the genomes of *Ochrobactrum*, *Thermotoga*, *Oceanithermus* and *Hoeflea*, suggest some variation of the reaction sequence. Here, obvious cupin homologs are missing, although all other genes of the proposed pathway are clustered on the genome together with other genes (*e.g.*, a conserved transketolase-like protein). For these organisms, it remains to be tested if methanethiol is indeed released during metabolism of MTR-1P (e.g by the transketolase-like protein) or whether the steps downstream of the RLP differ from the reductive release-reaction sequence proposed in this study.

We would like to note that LC-FTMS-metabolomics, as demonstrated here, is a powerful tool to elucidate microbial pathways and assign enzyme function on an organismal level, especially when potential substrates are not available and other methods such as transcriptomics and proteomics alone are inconclusive (*e.g.*, in case of a non-essential, housekeeping pathway with otherwise low enzyme activities as shown here). In combination with classical knock-out methods, LC-FTMS metabolomics provide a synergistic approach to assign enzyme functions on a whole cell level, and future efforts will focus on developing our knock-out metabolomics method into a more systematic platform. In conclusion, LC-FTMS-metabolomics allows a mostly unbiased view into metabolic reactions *in vivo*, thereby identifying *bona fide* reactions even when not all (physiological) determinants or constraints are known (*e.g.*, the unexpected involvement of a thiol-based reducing equivalent for the release of methanethiol).

Finally, the finding that RLPs of the *R. rubrum* group operate in an alternative MTA-degradation pathway adds another piece of information to the evolutionary puzzle of the biosphere's most abundant protein, RubisCO. All RLPs characterized so far have been reported to be involved in sulfur metabolism, suggesting an interesting evolutionary link between sulfur and carbon metabolism. However, whether this evolutionary relationship is simply based on the fact that the substrates for RubisCO and RLPs are structurally related, or if there is a more general connection between sulfur metabolism and carbon fixation in evolution will be the object of ongoing discussions[2,28–31].

METHODS

In extracto-NMR

For ^{1}H-NMR on cell extracts, cells growing on minimal medium with sulfate or MTA as sulfur source (100 ml scale, OD_{578}=0.5–0.8) were harvested by centrifugation (8,000×g, 10 min, 4 °C). Cells (0.3–0.5 g) were resuspended in 100 mM potassium phosphate in D_2O (0.4–0.7 ml, pD 7.8) and lysed by sonication on ice (20–30×5 s pulses, 1/8" microtip horn, 15% intensity, level 3, Misonix Ultrasonic Sonicator XL2020). Cell debris was pelleted by centrifugation (14,000×g, 10 min, 4 °C), and the protein concentration in the supernatant was determined according to Bradford using BSA as standard[32]. In some cases, the cell extract was additionally exchanged against buffer in D_2O by ultrafiltration-centrifugation using a 10 kDa exclusion membrane to remove excess traces of H_2O. $MgCl_2$ was added to a final concentration of 3–5 mM, and ^{1}H-NMR spectra of cell extracts (0.75–1.0 ml, 0.5–1.0 mg total protein) were acquired on a Varian Unity Inova 500 NB spectrometer (Varian, Palo Alto, CA) before and after adding MTA to the NMR tube (0.7–1.0 mM final concentration) every 30 min over a time course of 12–16 hours at 30 °C (number of transients per spectrum=256, 17 min acquisition time). Formation of MTR-1P and MTRu-1P from MTA was confirmed by the (dis)appearance of characteristic signals known from authentic standards To determine formation rates of MTR-1P and MTRu-1P, the relative concentrations of both compounds compared to the absolute concentration of MTA (0.9–1.1 mM) were quantified *via* integration of the characteristic methylthio proton-signal of each compound (D_2O/cell extract, 500 MHz, δ (in ppm) for the H_3CS-group of MTA=2.07 *s*; δ for H_3CS-group of MTR-1P=2.13 *s*; δ for H_3CS-group of MTRu-1P=2.09 *s*).

LC-FTMS metabolomics

Preparation of cells—Cells for metabolomics analysis were prepared from freshly grown cultures of *R. rubrum* wildtype and mutants (100 ml scale, OD_{578}=0.5–0.8) by centrifugation (4,000×g, 10 min, 4 °C). Cell pellets were washed by resuspension in 25–40 ml minimal medium without sulfur source, followed by centrifugation and resuspension in 3–5 ml of minimal medium without sulfur source. Then, the OD_{578} of these cell suspensions was adjusted to 6.0 with minimal medium without sulfur source, and incubated for 10 min at room temperature (22–24 °C). Cell suspension aliquots of 1 ml were prepared in eppendorf tubes and pelleted by centrifugation (14,000×g, 5 min, 22–24 °C). The supernatant was discarded, and cell pellets were kept on ice until start of the feeding experiment (or frozen away for direct metabolite extraction).

Feeding experiment—The cell pellet aliquots on ice were resuspended in 1 ml minimal medium without sulfur source (control samples), 1 ml minimal medium containing 1–2 mM MTA (feeding samples), or frozen directly in liquid nitrogen (t_0 samples). Cells were incubated for 2, 10, or 20 min at 30 °C, before pelleting by centrifugation (14,000×g, 90 s, 4 °C). The supernatant was decanted by strongly flicking the eppendorf tube. Cell pellets were immediately frozen away in liquid nitrogen, and samples were stored at −80 °C until further use.

Metabolite extraction and metabolite analysis—To extract metabolites, frozen cell pellets were resuspended in 0.375 mL 10 mM ammonium bicarbonate buffer (pH 9.2) containing 90% acetonitrile and then analysed immediately. LC-FTMS analysis was performed on the custom instrument described in the supplementary methods equipped with an Agilent 1200 HPLC system. Extracted metabolites were analyzed by injecting 100 μL of the sample onto a 2.1 X 150 mm Zic-HILIC column (Sequant) equilibrated with 10 mM ammonium bicarbonate buffer (pH 9.2) containing 90% acetonitrile (solvent B). Solvent consisted of 10 mM ammonium bicarbonate (pH 9.2). A linear gradient of 100%B to 40%B over 35 min then 40%B to 100%B in 10 min followed by a 15 min re-equilibration, at a flow rate 200 μL/min was used. All data were collected in negative profile mode at resolution 50,000 with full scan set to *m*/*z* 100–1000.

Data analysis—Data were analyzed using the software package SIEVE 1.3 (Vast Scientific). Default parameters were used except: max frames were set to 2000, threshold was set to 5000, and *m*/*z* tolerance was set to 0.001. Identification was performed using the Chemspider interface searched against the KEGG database. Peak lists were filtered to remove adducts and isotope peaks. Further filtering returned a peak list that showed significant change between the control and MTA fed samples (P value <0.01). The resulting peak list was exported to Microsoft Excel for relative quantitation using integrated intensities of the significant peaks. Manual analysis using the Qualbrowser application of Xcalibur (Thermo-Fisher Scientific) was performed on all automatically called significant peaks to remove missed isotopes, adducts, multimers, and erroneously called peaks. Peak identifications were corroborated using isotope pattern analysis and authentic standards as appropriate. Complementary data analysis was performed using the freely available software package XCMS[33] and a newly developed in-house program that will be released elsewhere. XCMS analysis used the group, rector and fillPeaks and groupval functions. XCMS results were then analyzed using our in-house software. Briefly, the XCMS called peaks were further refined through deisotoping and removal of adducts taking into account multimers as well as canonical adducts. Peaks were further filtered by retention time. Peaks less than 3.5 min or greater than 35 min were removed from the sample sets. Peaks that were statistically different between samples were ranked using One-Way ANOVA. Only peaks with a p-value less than 0.01 were selected for further analysis. Isotopes and their relative abundance were also investigated to calculate the possible elemental compositions of the intermediates. Accurate mass of the predicted top three formulas was used to search databases with a mass tolerance of 2 ppm. Database searches were performed using the online interface modules of KEGG (http://www.genome.jp/kegg/)[34], M E T L I N (http://metlin.scripps.edu/)[35], and

HMDB (http://www.hmdb.ca/)[36]. Search hits were compared with each other, and all analyses were manually validated.

Additional Methods

Information on bacterial strains and cultivation conditions, fine chemicals and syntheses, heterologous expression and purification of enzymes, mutagenesis, enzymatic and whole cell assays, as well as proteomics and transcriptomics is available in Supplementary Methods.

Supplementary Material

Refer to Web version on PubMed Central for supplementary material.

Acknowledgments

This research was supported by a fellowship to T.J.E. from the Deutsche Forschungs-gemeinschaft (ER 646/1-1) and research grants from the National Institutes of Health (R01GM065155, R01GM095742, P01GM071790, and U54GM093342). We would like to thank John E. Cronan for critical comments, and Caitilin Deane and Taka Miyairi for excellent technical assistance. We also acknowledge Steven C. Almo and Brandan S. Hillerich (New York Structural Genomics Research Consortium; NYSGRC) for providing expression plasmids and purified cupin for *in vitro* assays.

References

1. Phillips R, Milo R. A feeling for the numbers in biology. Proceedings of the National Academy of Sciences of the United States of America. 2009; 106:21465–21471.10.1073/pnas.0907732106 [PubMed: 20018695]
2. Tabita FR, et al. Function, structure, and evolution of the RubisCO-like proteins and their RubisCO homologs. Microbiology and Molecular Biology Reviews. 2007; 71:576.10.1128/mmbr.00015-07 [PubMed: 18063718]
3. Hanson TE, Tabita FR. A ribulose-1,5-bisphosphate carboxylase/oxygenase (RubisCO)-like protein from *Chlorobium tepidum* that is involved with sulfur metabolism and the response to oxidative stress. Proceedings of the National Academy of Sciences of the United States of America. 2001; 98:4397–4402. [PubMed: 11287671]
4. Ashida H, et al. A Functional Link Between RuBisCO-like Protein of *Bacillus* and Photosynthetic RuBisCO. Science. 2003; 302:286–290.10.1126/science.1086997 [PubMed: 14551435]
5. Imker HJ, Singh J, Warlick BP, Tabita FR, Gerlt JA. Mechanistic diversity in the RuBisCO superfamily: a novel isomerization reaction catalyzed by the RuBisCO-like protein from *Rhodospirillum rubrum*. Biochemistry. 2008; 47:11171–11173.10.1021/bi801685f [PubMed: 18826254]
6. Pearce FG. Catalytic by-product formation and ligand binding by ribulose bisphosphate carboxylases from different phylogenies. Biochem J. 2006; 399:525–534. BJ20060430 [pii]. 10.1042/BJ20060430 [PubMed: 16822231]
7. Cleland WW, Andrews TJ, Gutteridge S, Hartman FC, Lorimer GH. Mechanism of Rubisco: The Carbamate as General Base. Chem Rev. 1998; 98:549–562. cr970010r [pii]. [PubMed: 11848907]
8. Paech C, Pierce J, McCurry SD, Tolbert NE. Inhibition of ribulose-1,5-biphosphate carboxylase/oxygenase by ribulose-1,5-bisphosphate epimerization and degradation products. Biochem Biophys Res Commun. 1978; 83:1084–1092. [PubMed: 708427]
9. Imker HJ, Fedorov AA, Fedorov EV, Almo SC, Gerlt JA. Mechanistic diversity in the RuBisCO superfamily: the “enolase” in the methionine salvage pathway in *Geobacillus kaustophilus*. Biochemistry. 2007; 46:4077–4089.10.1021/bi7000483 [PubMed: 17352497]

10. Carre-Mlouka A, et al. A new rubisco-like protein coexists with a photosynthetic rubisco in the planktonic cyanobacteria *Microcystis*. J Biol Chem. 2006; 281:24462–24471. M602973200 [pii]. 10.1074/jbc.M602973200 [PubMed: 16737967]
11. Sekowska A, et al. Bacterial variations on the methionine salvage pathway. BMC Microbiology. 2004; 4:9. [PubMed: 15102328]
12. Albers E. Metabolic characteristics and importance of the universal methionine salvage pathway recycling methionine from 5′-methylthioadenosine. IUBMB Life. 2009; 61:1132–1142.10.1002/iub.278 [PubMed: 19946895]
13. Singh J, Tabita FR. Roles of RubisCO and the RubisCO-like protein in 5-methylthioadenosine metabolism in the Nonsulfur purple bacterium *Rhodospirillum rubrum*. J Bacteriol. 2010; 192:1324–1331. JB.01442-09 [pii]. 10.1128/JB.01442-09 [PubMed: 20038587]
14. Sekowska A, Mulard L, Krogh S, Tse JK, Danchin A. MtnK, methylthioribose kinase, is a starvation-induced protein in Bacillus subtilis. BMC Microbiol. 2001; 1:15. [PubMed: 11545674]
15. Sekowska A, Robin S, Daudin JJ, Henaut A, Danchin A. Extracting biological information from DNA arrays: an unexpected link between arginine and methionine metabolism in Bacillus subtilis. Genome biology. 2001; 2:1–12.
16. Sekowska A, Danchin A. The methionine salvage pathway in Bacillus subtilis. BMC Microbiol. 2002; 2:8. [PubMed: 12022921]
17. Ellman GL. Tissue sulfhydryl groups. Arch Biochem Biophys. 1959; 82:70–77. [PubMed: 13650640]
18. Fagerbakke KM, Heldal M, Norland S. Content of carbon, nitrogen, oxygen, sulfur and phosphorus in native aquatic and cultured bacteria. Aquat Microb Ecol. 1996; 10:15–27.
19. Paulin LG, Brander EE, Poso HJ. Specific inhibition of spermidine synthesis in Mycobacteria spp. by the dextro isomer of ethambutol. Antimicrobial agents and chemotherapy. 1985; 28:157–159. [PubMed: 4037776]
20. Gopishetty B, et al. Probing the catalytic mechanism of S-ribosylhomocysteinase (LuxS) with catalytic intermediates and substrate analogues. J Am Chem Soc. 2009; 131:1243–1250. 10.1021/ja808206w [pii]. 10.1021/ja808206w [PubMed: 19099445]
21. Kiene RP, Linn LJ, Gonzalez J, Moran MA, Bruton JA. Dimethylsulfoniopropionate and methanethiol are important precursors of methionine and protein-sulfur in marine bacterioplankton. Appl Environ Microbiol. 1999; 65:4549–4558. [PubMed: 10508088]
22. Bolten CJ, Schroder H, Dickschat J, Wittmann C. Towards methionine overproduction in *Corynebacterium glutamicum* - methanethiol and dimethyldisulfide as reduced sulfur sources. J Microbiol Biotechnol. 2010; 20:1196–1203. JMB020-08-06 [pii]. [PubMed: 20798582]
23. Rohmer M, Knani M, Simonin P, Sutter B, Sahm H. Isoprenoid Biosynthesis in Bacteria - a Novel Pathway for the Early Steps Leading to Isopentenyl Diphosphate. Biochemical Journal. 1993; 295:517–524. [PubMed: 8240251]
24. Eisenreich W, Bacher A, Arigoni D, Rohdich F. Biosynthesis of isoprenoids via the non-mevalonate pathway. Cell Mol Life Sci. 2004; 61:1401–1426.10.1007/s00018-004-3381-z [PubMed: 15197467]
25. Hamana K, Kamekura M, Onishi H, Akazawa T, Matsuzaki S. Polyamines in photosynthetic eubacteria and extreme-halophilic archaebacteria. J Biochem. 1985; 97:1653–1658. [PubMed: 3928615]
26. Hamana K, Matsuzaki S. Polyamines as a chemotaxonomic marker in bacterial systematics. Critical reviews in microbiology. 1992; 18:261–283.10.3109/10408419209113518 [PubMed: 1524675]
27. Salim HM, Negritto MC, Cavalcanti AR. 1+1 = 3: a fusion of 2 enzymes in the methionine salvage pathway of Tetrahymena thermophila creates a trifunctional enzyme that catalyzes 3 steps in the pathway. PLoS genetics. 2009; 5:e1000701.10.1371/journal.pgen.1000701 [PubMed: 19851454]
28. Ashida H, et al. RuBisCO-like proteins as the enolase enzyme in the methionine salvage pathway: functional and evolutionary relationships between RuBisCO-like proteins and photosynthetic RuBisCO. J Exp Bot. 2008; 59:1543–1554.10.1093/jxb/ern104 [PubMed: 18403380]

29. Tabita FR, Hanson TE, Satagopan S, Witte BH, Kreel NE. Phylogenetic and evolutionary relationships of RubisCO and the RubisCO-like proteins and the functional lessons provided by diverse molecular forms. Philos T R Soc B. 2008; 363:2629–2640.10.1098/rstb.2008.0023

30. Tabita FR, Satagopan S, Hanson TE, Kreel NE, Scott SS. Distinct form I, II, III, and IV Rubisco proteins from the three kingdoms of life provide clues about Rubisco evolution and structure/function relationships. Journal of Experimental Botany. 2008; 59:1515–1524.10.1093/jxb/erm361 [PubMed: 18281717]

31. Ashida H, Danchin A, Yokota A. Was photosynthetic RuBisCO recruited by acquisitive evolution from RuBisCO-like proteins involved in sulfur metabolism? Research in microbiology. 2005; 156:611–618.10.1016/j.resmic.2005.01.014 [PubMed: 15950120]

32. Bradford MM. A rapid and sensitive method for the quantitation of microgram quantities of protein utilizing the principle of protein-dye binding. Anal Biochem. 1976; 72:248–254. S0003269776699996 [pii]. [PubMed: 942051]

33. Smith CA, Want EJ, O'Maille G, Abagyan R, Siuzdak G. XCMS:Processing Mass Spectrometry Data for Metabolite Profiling Using Nonlinear Peak Alignment, Matching, and Identification. Analytical Chemistry. 2006; 78:779–787.10.1021/ac051437y [PubMed: 16448051]

34. Kanehisa M, et al. From genomics to chemical genomics: new developments in KEGG. Nucleic Acids Res. 2006; 34:D354–357.10.1093/nar/gkj102 [PubMed: 16381885]

35. Smith CA, et al. METLIN: a metabolite mass spectral database. Therapeutic drug monitoring. 2005; 27:747–751. [PubMed: 16404815]

36. Wishart DS, et al. HMDB: a knowledgebase for the human metabolome. Nucleic Acids Res. 2009; 37:D603–610.10.1093/nar/gkn810 [PubMed: 18953024]

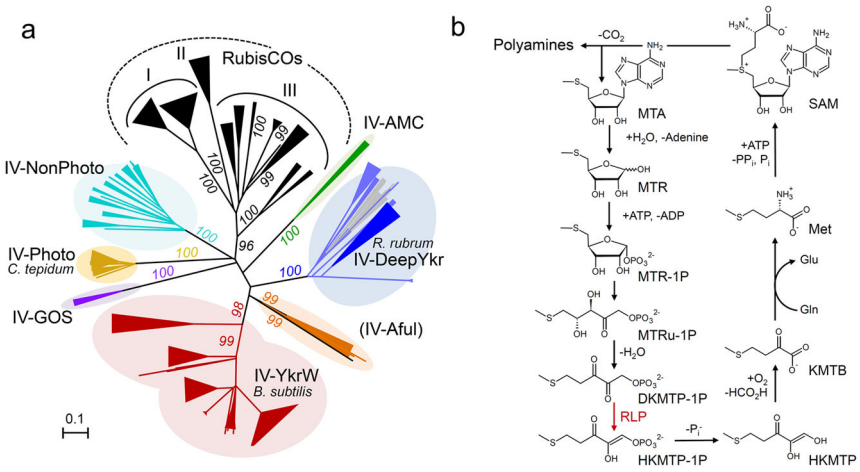

Fig. 1. Phylogeny and function of RLPs

(**A**) Phylogenetic tree of the RubisCO/RLP superfamily. The unrooted phylogenetic tree is based on amino acid sequence analysis of 333 representative proteins (listed in Supplementary Table 6) that were restricted to a length of 409 amino acids and aligned with ClustalW. Tree topography and evolutionary distance are given by the neighbor joining method. Numbers at nodes represent the percentage bootstrap values for the clades of this group in 500 replications. Similar trees were obtained by using the minimum evolution and the maximum likelihood method. For extended views of each subtree, see Supplementary Fig. 12 and 13. The scale bar represents a difference of 0.1 substitutions per site. RubisCOs are classified into three well established subfamilies[2,29] (I, II and III). RLPs fall into six different subfamilies as described previously[2,29]: IV-AMC (metagenomic *Leptospirillum* sequences from an acid mine consortium); IV-DeepYkr; (*R. rubrum* group, including mainly alpha-, and gammaproteobacteria, some thermophilic species and Veillonellaceae); IV-YkrW (*B. subtilis* group, including many Bacilliales, Acidithiobacillales, and cyanobacteria); IV-GOS (metagenomic sequences from the global ocean sequencing program); IV-Photo (*C. tepidum* group, including many Chlorobiales and alphaproteobacteria,) and IV-NonPhoto (including many alpha-, and some beta proteobacteria). A seventh subgroup of RLPs, established in this extended phylogenetic analysis (IV-Aful, including Clostridiales and *Archaeoglobus fulgidus*) was described previously as a singleton (*A. fulgidus* DSM 4304) [2]. (**B**) Function of the *B. subtilis* RLP in the classical methionine salvage pathway. Abbreviations: MTR, methylthioribose; DKMTP-1P, 2,3-diketo-5-methylthiopentyl-1-phosphate; HKMTP-1P, 2-hydroxy-3-keto-5-methylthiopentenyl-1-phosphate; HKMTP 1,2-dihydroxy-3-keto-5-methylthiopentene; KMTB, 2,4-keto-4-methylthiobutyrate.

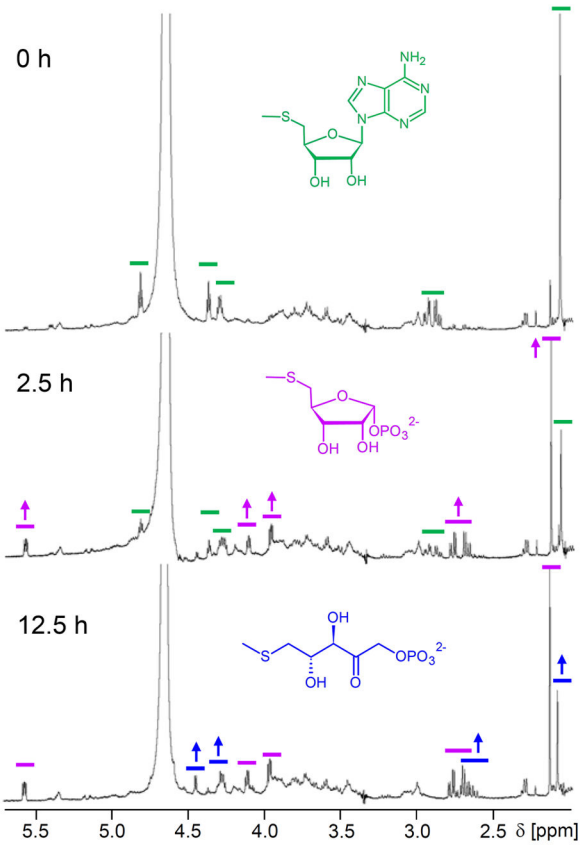

Fig. 2. Characterization of the initial steps in MTA-metabolism of *R. rubrum* by *in-extracto* NMR

^{1}H-NMR spectra of *R. rubrum* cell extract incubated with MTA that show the transformation of MTA into MTR-1P, and MTRu-1P over time. 0.78 mg cell extract protein of *R. rubrum* grown on MTA as sole sulfur source were incubated with 0.4 mM MTA at 30 °C. Spectra were recorded at different time points as indicated. Characteristic ^{1}H-NMR signals for MTA (green), MTR-1P (purple), and MTRu-1P (blue) are indicated by colored lines. The full array experiment is shown in Supplementary Figure 1.

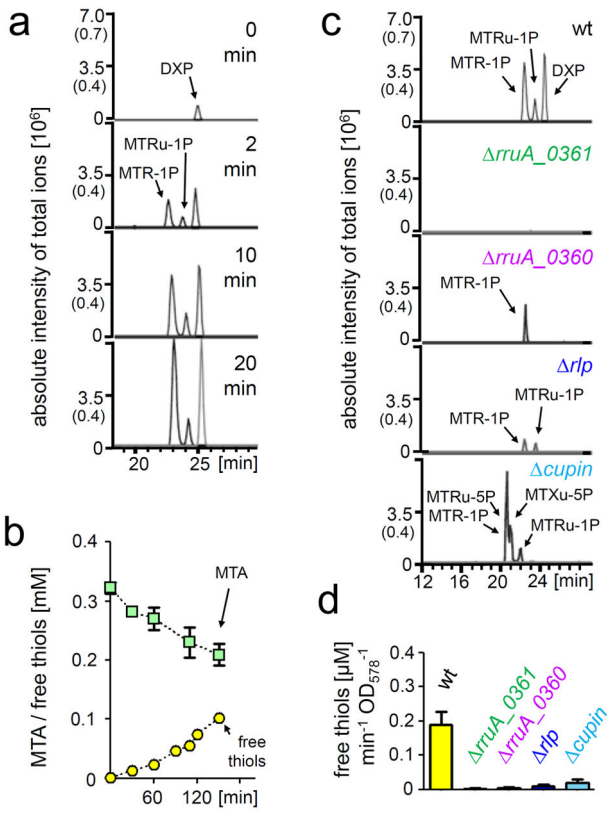

Fig. 3. Methanethiol release and DXP formation are linked in *R. rubrum*

(**A**) Time-dependent formation of intermediates in the MTA-isoprenoid shunt upon MTA-feeding. Cell suspensions of *R. rubrum* (1 ml, $OD_{578=}$6.0) were incubated with 0.4 mM MTA and analyzed after 2, 10, and 20 minutes respectively by LC-FTMS-metabolomics. (**B**) Time dependent formation of free thiols by *R. rubrum* upon MTA uptake. Cell suspensions of *R. rubrum* (1 ml, OD_{578}=4.0) were incubated with 0.4 mM MTA. The supernatant was analyzed for consumption of MTA and formation of free thiols. Free thiols formed were identified as methanethiol by HPLC and FTMS (Supplementary Fig. 4). At least two independent cell batches were used in these assays. Data represent mean values ± standard deviation. (**C**) LC-FTMS-Metabolomics analysis of MTA-isoprenoid shunt mutants. Cell suspensions of *R. rubrum* wild type and different mutants were incubated with MTA (according to **A**) and analyzed after 10 minutes by LC-FTMS-metabolomics, see Supplementary Fig. 6 for the detailed analysis of the *cupin* mutant (**D**) Thiol release activities by *R. rubrum* wild type and different mutants. Cell suspensions of *R. rubrum* were incubated with MTA according to (**B**), and the formation of free thiols over time was quantified. At least two independent cell batches were used in these assays. Data represent mean value ± standard deviation.

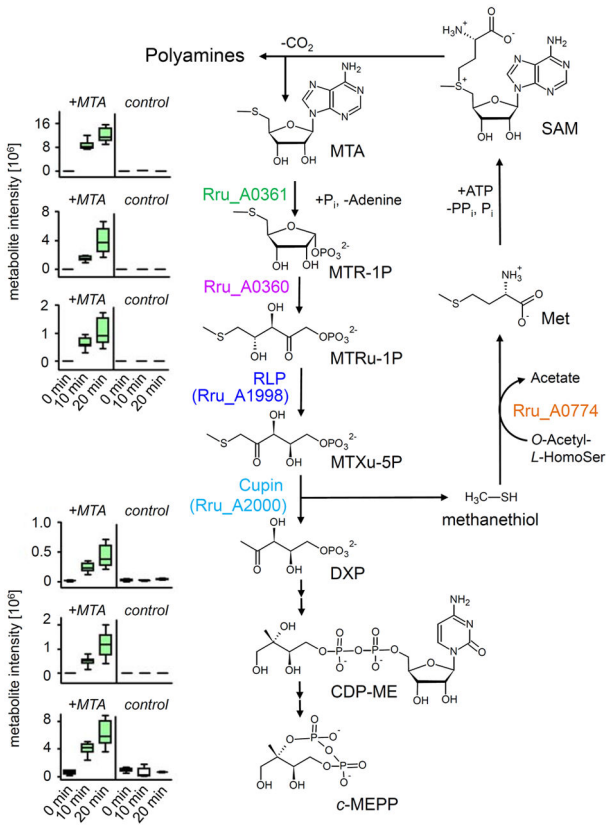

Fig. 4. The proposed MTA-isoprenoid shunt in *R. rubrum*

The RLP is part of the central reaction sequence that involves the release of methanethiol from the molecule backbone. Whereas methanethiol can be recaptured as methionine *via O*-acetyl-*L*-homoserine sulfhydrylase (Rru_A0774), the rest of the molecule is converted into isoprenoid precursors. All intermediates of this proposed pathway that were identified by LC-FTMS-metabolomics are shown in boxed bar charts, with their individual increase in metabolite level after 0, 10 and 20 minutes feeding of MTA (*+MTA*, green bars) in comparison to control cells after 0, 10 and 20 min (*control*, black bars). Genes/proteins that were identified and characterized in this study are also shown and highlighted by colors.

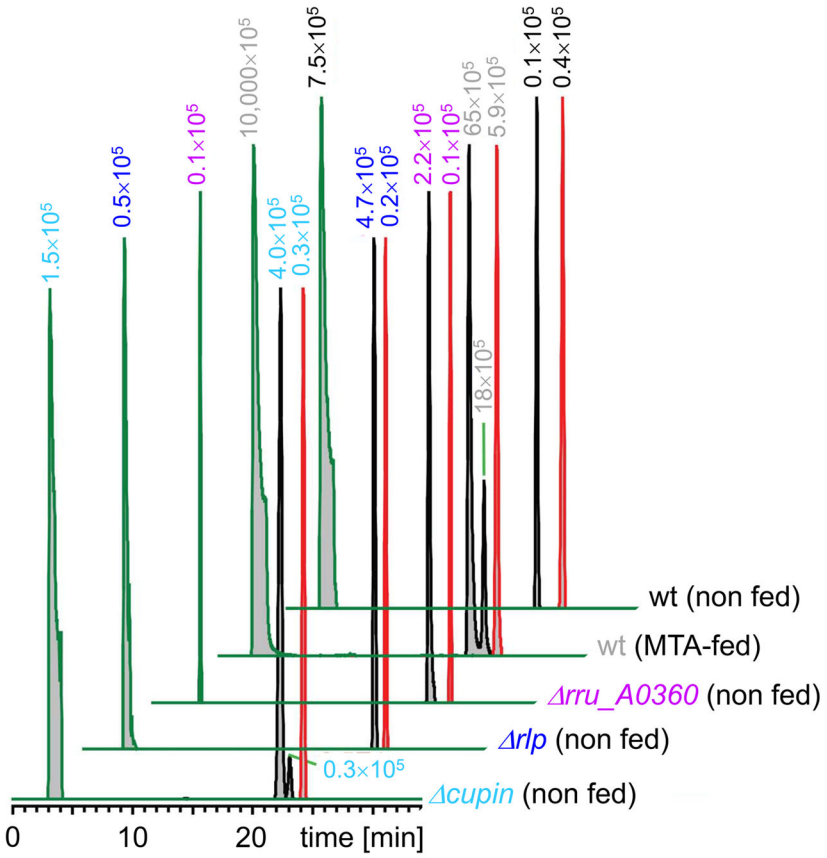

Fig. 5. Analysis of MTA derived metabolites in *R. rubrum* wildtype and mutants without feeding of external MTA

Metabolite extracts prepared from *R. rubrum* wildtype cells and mutants that had been cultivated on minimal medium with sulfate as sole sulfur source were analyzed for intermediates of the proposed MTA-isoprenoid shunt. The data are represented by extracted ion chromatograms (negative ion) at 2 ppm mass accuracy for 296.08228 (MTA; retention time 3.5 min; green traces), 259.00468 (methylthiopentose phosphates: MTR-1P, MTRu-1P, MTXu-5P, and MTRu-5P; retention time 22–23 min; black traces), and 213.01696 (DXP; retention time 24.5 min; red traces). The integrated intensities are inset and color coded for each sample. Note that the single traces are scaled to 100% relative intensity. For comparison, integrated intensities are also summarized in Supplementary Table 7.

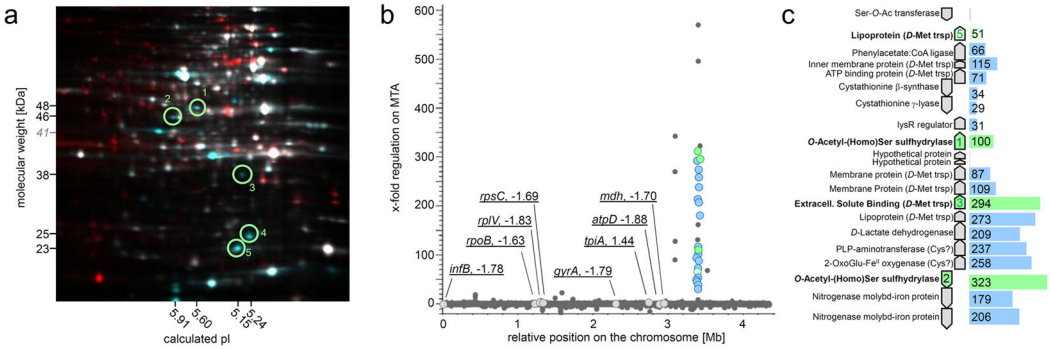

Fig. 6. Proteome and transcriptome analysis of *R. rubrum* cells that were grown aerobically with sulfate or MTA as sole sulfur source

(**A**) Differential induced gel electrophoresis (DIGE) analysis of changes in the proteome of *R. rubrum*. Proteins up-regulated in MTA-grown cells are shown in cyan, proteins up-regulated in sulfate-grown cells are shown in red, whereas proteins that are not changed under both conditions are shown in white. The calculated pI (first dimension) and the molecular mass standards (second dimension) of the DIGE gel are given. For more information on the five proteins highlighted in green that were selected for identification, see Supplementary Table 4. (**B**) RNA sequencing (RNAseq) analysis of changes in the transcriptome of *R. rubrum*. Genes annotated on the chromosome of R. rubrum, are represented by dots according to their physical location on the chromosome and their fold change in mRNA-level. Classical housekeeping genes are listed separately and highlighted by light gray dots in the graph. For more information on all transcripts up-regulated more than 30-fold, see Supplementary Table 5. (**C**) The “thiol cluster” that was identified by both DIGE and RNAseq analysis. The four proteins of the thiol cluster that were identified by DIGE are numbered and highlighted in green. Transcripts of the thiol-cluster that were identified by RNAseq. are highlighted in cyan, and the fold-upregulation of each gene is given separately.